Journal of Trace Elements in Medicine and Biology 73 (2022) 127029

Contents lists available at ScienceDirect

Journal of Trace Elements in Medicine and Biology

journal homepage: www.elsevier.com/locate/jtemb

Neodymium oxide nanostructures and their cytotoxic evaluation in human cancer cells

Javed Ahmad [a,*], Rizwan Wahab [a,b], Maqsood A. Siddiqui [a], Nida Nayyar Farshori [c], Quaiser Saquib [a,b], Naushad Ahmad [d], Abdulaziz A. Al-Khedhairy [a,b]

[a] Chair for DNA Research, Zoology Department, College of Sciences, King Saud University, Riyadh 11451, Saudi Arabia
[b] Zoology Department, College of Sciences, King Saud University, Riyadh 11451, Saudi Arabia
[c] Department of Pharmacognosy, College of Pharmacy, King Saud University, Riyadh 11495, Saudi Arabia
[d] Department of Chemistry, College of Science, King Saud University, Riyadh 11451, Saudi Arabia

ARTICLE INFO

Key words:
Neodymium oxides
TEM
MTT
NRU
ROS
Cell lines

ABSTRACT

Neodymium oxide exhibits a unique property, which facilitates and largely utilized as an industrial applications. A number of cytotoxic study is available but very limited information is available to understand their biological activity with neodymium oxide at a very low conc- entration of the material. The present work was designed to understand the cytotoxicity against liver (HepG-2) and lung (A-549) cancer cells. Initially, Neodymium oxides (Nd_2O_3) were prepared and characterized with various instruments. The crystallinity and morphology of Nd_2O_3 powder were examined with instruments such as X-Ray Diffraction (XRD), scanning electron microscope (SEM), Transmission electron microscopy (TEM), Energy Dispersive X-Ray Analysis (EDX) respectively, revealed the size of curved nanostructure are ~140 ± 2 in diameter whereas length goes upto ~700 nm with elemental composition. The cytotoxicity study was conducted with MTT, NRU assay with genotoxicity study via ROS, cell cycle and qPCR analysis. The cells cytotoxic assessment were analysed via MTT(3-(4,5-Dimethylthiazol-2-yl)−2,5-Diphenyl tetra zolium Bromide) and Neutral Red Uptake (*NRU*) assay with neodymium oxide (Nd_2O_3), which indicates the reduction in cell viability. Additionally, cell-cycle analysis showed an increase in the apoptotic peak after a 24-h. Quantitative real-time PCR (RT-PCR) data revealed that apoptotic genes such as p53, bax, and caspase-3 were up regulated, whereas bcl-2, an anti-apoptotic gene, was down regulated; therefore, apoptosis was mediated through ROS and genotoxicity pathways. The experiments of cytotoxicity was tested and concludes that the Nd_2O_3 express a moderate and dose dependent effect on cancer cells. The ROS, cell cycle analysis and qPCR showed that Nd_2O_3 exhibit the capability to cells death via ROS generation and genotoxicity study pathways.

1. Introduction

A series of rare-earth metals, which are identified in the periodic table are toxic in nature and affected directly or indirectly to the environment and human beings [1–3]. Roles of rare earth elements focusing on different organisms exposure, points to a series of adverse effects including bioaccumulation, respiratory diseases etc. [4]. Although, this is well known and studied the chemical toxicity of the materials but its very limited and not well explored on the effect human biological systems [5]. The nanotechnology fascilitates to understand the role of nanostructured material towards the direction of human beings [6,7]. Among various rare metals, the neodymium is one of the rare earth elements (REEs), inclued in 17 metal elements (15 lanthanides & 2 non-lanthanides) and shares similar physicochemical and related properties [8–10]. Due to their unique magnetic properties [11], neodymium is used as a permanent magnets [12], loud speakers [13], audio systems [14], headphones [15], hard drives [16] in computers, catalysts [17], turbines [18] etc. The global demand of neodymium is increases

Abbreviations: MTT, 3-(4,5-Dimethylthiazol-2-yl)-2,5-Diphenyl tetra zolium Bromide); NRU, Neutral Red Uptake; ROS, Reactive oxygen Species; Nd_2O_3, Neodymium oxides; XRD, X-Ray Diffraction; SEM, scanning electron micro scope; TEM, Transmission electron microscopy; EDX, Energy Dispersive X-Ray Analysis; qPCR, Quantitative real-time PCR.

* Corresponding author.
E-mail addresses: javedbiochem@gmail.com, javedahmad@ksu.edu.sa (J. Ahmad).

https://doi.org/10.1016/j.jtemb.2022.127029
Received 29 December 2021; Received in revised form 15 June 2022; Accepted 22 June 2022
Available online 23 June 2022

rapidely and the annual production turnover is 7300 tons, which accounts as a fourth largest REEs production in the world [19,20].

Several physicochemical methods were applied to synthesis the Nd_2O_3 as a bulk nano structure or thin film such as chemical vapour deposition (CVD) [21], plasma chemical vapour deposition (PECVD) [22], thermal deposition [23], chemicals, mechanical and other approches [24]. The material can also be prepared via a low cost and easy processing ways such as inverse microemulsion [25], sol-gel [26], ionic liquid surfactant templates [27], hydrothermal [28], auto combustion [29], sono chemical [30] etc. Among various ways of preparation procedure for the formation of Nd_2O_3 chemical precipitation process is the best method also cost effective and can be synthesize Nd_2O_3 in bulk amount [30].

The physical exposure to the human beings is toxic, whereas limited studies available to expose the prepared nanostructured against cells lines such as a long range of REEs trichloride salts (Y(III), La(III),Ce(III), Nd(III), Sm(III), Eu(III) and Gd(III)) were used for the cytotoxicity study and it shows the developmental defects *Para-centrotuslividus pluteus larvae* with the following exposure [31]. In another report published by Blaise et al., shows the REEs ecotoxicity responses generated with *Hydra attenuata*, also known as *Hydra vulgaris*, an animal model used extensively. They showed that the Hydra toxicity responses to REEs to be among the most sensitive, along with those of other invertebrate species [32]. In another work, the angiogenic processes was explored and check the effect with neodymium NPs in modulating blood vessel formation via angiogenic for strategy to identify a biocompatible nano therapeutics for treating diseases [33]. The rat NR8383 alveolar macrophages were also used to test cytotoxicity study with Nd_2O_3 and showed that the material was toxic and was dose dependent [34]. Chen et al., explained that the toxic effects of Nd_2O_3 NPs on early development of *Zebrafish Embryos* [35]. The result express that the Nd_2O_3 activated the apoptosis pathway and induces toxicity with abnormal cardiac/cerebrovascular developments [35]. The bio chemical alterations were also studied by Nd at different concentrations (2.5, 5, 10, 20 and 40 mg/L) in the mussel (*Mytilus galloprovincialis*) exposed to this element for 28 days [36]. Recently, the neodymium nanorods were synthesized and characterized for the nano carrier through coating them with a poly-β-cyclodextrin polymer and possible to apply as an anticancer drug delivery studies and photothermal therapy [37]. In other work, the alloys of Neodymium (NdFeTi and two NdFeSi alloys) were applied for *in vitro* study with two model organisms (the A549 human cell line and the yeast *Saccharomyces cerevisiae*) for both viability and oxidative stress assays. The study explained that the direct alloys are harmful effects also their toxicological details were compared with other reference materials [38]. In another work, cytotoxic and radio sensitization ability for Nd_2O_3NPs was checked with mammalian cell lines; U-87 MG and Mo59K. A significant change in cytotoxicity and autophagy were observed in U-87 MG cells once exposed Nd_2O_3 and La_2O_3. The study indicates the importance of the genotype of cells with the use of rare earth oxides [39]. Among various biological studies with Nd_2O_3 nanostructures such as particles and other various shaped structures, limited study is available on the human cells lines such as a liver, lung and others.

Liver, which is a metabolic organ in the body and it's directly and indirectly affected with the environment, whereas the lung, which inhales various types of toxic gases and pollutions and a very important organ in the body. Due to their important function in the body and daily exposure to the environment, we have chosen liver (HepG-2) and lung (A-549) cancer cells lines, which are widely accepted in the world and their exposure with prepared curved shaped neodymium oxide (Nd_2O_3) for their cytotoxic evaluation against both cancer cell lines [40,41]. The objective of the present study is to investigate the effect of Nd_2O_3 on human cell line of HepG-2 and A-549 cells by measuring cell viability with different concentrations of Nd_2O_3. The novelty of the present work describes here that although a number of studies are available related to the cytotoxicity with human cell line of HepG-2 and A-549 cells but there is no data available which show the cytotoxicity studies with human cell line of HepG-2 and A-549 cells by measuring cell viability with very low concentrations of Nd_2O_3. These findings may provide further insight into the cytotoxicity of rare earth Nd_2O_3 and the roles of Nd_2O_3 in human cell toxicity, which could benefit the Nd_2O_3 industrial standard and safety standard formulation. The Nd_2O_3 was synthesized via solution method and characterized well with various tools such as X-ray diffraction pattern was employed to know the crystallinity of the material. The scanning electron microscopy (SEM) was used to know the general morphology of prepared material equipped with the EDX, which displayed the elemental proportion of the Nd_2O_3. Further the structural examination was conducted with TEM. The chemical functional and optical behaviors of the material were accessed via FTIR and UV–visible spectroscopy respectively. The cells morphology was examined via microscopy, whereas the cytotoxicity tests were measured via MTT and NRU assays. The reactive oxygen species (ROS) generation, Cell cycle analysis, and RT-PCR study, was also performed. Based on the acquired results and their analysis a possible discussion was explained here.

2. Material and methods

2.1. Synthesis of curved shaped nanostructure of neodymium oxide

The Neodymium oxide nanostructures were prepared with use of Neodymium nitrate ($Nd(NO_3)_2.6H_2O$) and sodium hydroxide (NaOH) purchased from Sigma Aldrich Chem corporation and used without any further purification. The 0.25 M ($Nd(NO_3)_2$ $6H_2O$) was dissolved in 100 mL of beaker. Once the dissolution was completed, to this NaOH (0.3 M in 100 mL) was poured and mixed gently. The solutions pH was measured and it was reached to 12.73. The mixture was transferred to the refluxing pot and heated at 90ºC for 3 h. When the reaction was completed aqueous product was centrifuged (4000 rpm for 3 min) to eliminate the ionic impurities and thereafter it was transferred on to glass petri dishes and dried at 60ºC in an oven. The dried powder product was stored for further chemical, physical and biological analysis.

2.2. Characterization of prepared materials of neodymium oxide

The formed nanostructured powder crystallinity, phases, full width half maxima and other related information were identified via X-ray powder diffractometer (XRD) (PANalytical XPert Pro, U.S.A.) with $Cu_{K\alpha}$ radiation ($\lambda = 1.54178$ Å) in range of 20–70º with 6º/min scanning speed. The synthesized powder was analyzed to know their morphology with using scanning electron microscopy (SEM, JSM-6380, Japan). The analysis was conducted with prepared powders and it was squirted on the carbon tape and fixed it on the sample (Nd_2O_3) holder. Once the sampling was completed, the sample holder was transferred to a glass chamber and sputtered with thin conducting layer of platinum (pt) for 3 *s* for to enhance the conductivity of Nd_2O_3 material. The sample holder was fixed to SEM instrument and analyzed. Including the morphology, the elemental analysis (Energy Dispersive X-Ray Analysis (EDX)) was also performed to know the elements present in the materials and its equipped with SEM. For more clarification, the morphological evaluation was also accomplished via transmission electron microscopy (TEM, JEOL, JSM 2010, Japan) and the structural detail was recovered at 100 kV current. For the functional groups evaluation of used chemicals, FTIR spectroscopy was utilized in range of 400–4000 cm^{-1}. The analysis of FTIR spectroscopy was conducted with very small amount of the processed powder and it was mixed with KBr to form pellet under high-pressure (~4 *tons*). The pellet was fixed to the sample holder and analyzed the FTIR spectroscopy. The optical property of the material was also analyzed via UV–visible (UV–visible, Shimazu) spectroscopy ranges from 200 to 600 nm at room temperature.

2.3. Cell culture of liver (HepG-2) and lung (A-549) cancer cells with treatment of neodymium oxide

The liver (HepG-2) and lung cancer cells (A-549) were cultured in a specified medium (DMEM/MEM) with 10–12% fetal bovine serum (FBS), 0.2% sodium bicarbonate, and antibiotic-antimycotic solution (100X, 1 mL/100 mL of medium) with humid atmosphere (5% CO_2 & 95% O_2) at 37 °C. Earlier for the experiments, the cells viability were evaluated by trypan blue dye as per the protocol [42] and shows the viability more than 95% were only used in the study. The cells were employed between 10 and 12 passages to treat cells with nano structures. The material was initially used at high concentration and thereafter, it was diluted at desired and different concentrations for the treatment with cancer cells. The cells were grown in 6-well or 96-well plates as per the experiment requirement.

2.4. Reagents and consumables for the biological study

The MTT [3-(4, 5-dimethylthiazol-2-yl)-2, 5 diphenyltetrazolium bromide], was procured from Sigma Chemical Company Pvt. Ltd. St. Louis, MO, USA and used without any further modification except dilution, besides this the Dulbecco's Modified Eagle Medium (DMEM) and MEM culture medium, antibiotics-antimycotic and fetal bovine serum (FBS) were purchased from Invitrogen, USA. The plastic wares and other consumables products for the cells culture were used from Nunc, Denmark.

2.5. MTT assay

The viability of cells was examined via MTT assay for control and treated samples as per the previously set protocol [43]. In brief, the cells were initially cultured in a specialized 96 well plates (rate of 1×10^4/well) and it was incubated for 24 h at 37 °C with humidified environment. The cells were treated with prepared sample Nd_2O_3 from a long range of concentration (2.5–100 μg/mL) for 24 h. Once the cells were completely mixed in well plates, stock solution of MTT (5 mg/mL in PBS) was amalgamated with the rate of 10 μL/well in 100 μL of cell suspension and further incubated for 4 h. Once the incubation period was completed, the well plates solution was washed with PBS and in these wells ~200 μL of DMSO was added for to aspirate the formazan product and mixed gently. The optical analysis of the solution was measured at 550 nm using multiwall micro-plate reader (Multiskan Ex, Thermo Scientific, Finland). The control cells were employed as a reference and to run with the same conditions. The maximum absorbance depends upon the employed solvent in sample solution and the level of viability of cells % was calculated as per the equations mentioned below:

$$\% \text{ viability} = [(\text{total cells-viable cells})/\text{total cells}] \times 100$$

2.6. NRU assay

The assessment of toxicity for control and treated (Nd_2O_3) cancer cells were also performed via NRU assay as described previously [44,45]. Both cancer cells were seeded (10, 000/well) in 96 well plates. When the cells were completely grown (after 24 h), exposed it with the material at desired concentration (1–50 μg/mL) and reserved it for 24 h in an incubator. After the exposure, cells were further incubated in NR medium (50 μg/mL) for 3 h and thereafter cells were washed and dye was extracted in 1% acetic acid and 50% ethanol solution. The develop color was analyzed at 540 nm.

2.7. Reactive Oxygen Species (ROS) Generation

The generation of reactive oxygen species (ROS) was examined with using 2, 7-dichloro dihydro fluoresce in diacetate (DCFH-DA; Sigma Aldrich, USA) dye, which is utilized as a fluorescent agent. This was analyzed as per the previously described protocol [46]. The cells were exposed with the processed material for 24 h, and washed well with PBS and incubated for 30 min in DCFH-DA (20 μM) in dark medium at 37°C. Once the reaction of DCFH-DA with control and treated cells were completed, it was analyzed with intra-cellular fluorescence using fluorescence microscope.

2.8. Cell cycle analysis treated with Nd_2O_3

For the cell cycle analysis, HepG2 cells treated with increasing concentrations of Nd_2O_3 (25–200 μg/mL) for 24 h. Cells were centrifuged at 3000 rpm for 5 min, then pellet was washed thrice with cold PBS. Cells were fixed with 500 μL of chilled 70% ice-cold ethanol, incubated at 4 °C for 1 h. After washing, the pellet was suspended in PBS and stained with propiodium iodide (50 μg/mL) solution having 0.1% Triton X-100 and 0.5 mg/mL RNase A for 1 h in dark at 37 °C. The red fluorescence of 10,000 events of propiodium iodide (PI) stained cells were acquired in FL4 Log channel through a 675 nm filter using flow cytometer. The data were examined eliminating the cell debris, characterized by a low FSC/SSC, using the Beckman Coulter flow cytometer (Coulter Epics XL/Xl-MCL, USA and System II Software, Version 3.0).

2.9. Isolation of total RNA and real-time PCR (RT-PCR)

RNA was purified from 3×10^5 cells/well of HepG2 cells untreated and treated with Nd_2O_3 (200 μg/mL) for 24 h using the RNeasy mini Kit (Qiagen) as the manufacturer's protocol. Total RNA purity were verified by using Nanodrop 8000 spectrophotometer (Thermo Scientific, USA) and the integrity of RNA was visualized on 2% agarose gel using the documentation system (Universal Hood II, BioRad, USA). The cDNA was synthesized by the MLV reverse transcriptase (GE Health Care, UK) according to the kit instruction taking 2 μg of RNA and 100 ng of oligo $(dT)_{12–18}$ primer. For the quantification of set of primers of apoptotic and anti-apoptotic gene was done using Roche® LightCycler®480 (96-well block), following the recommended cycling program. For the reaction mixture of 20 μL taking 100 ng of the cDNA and 7.5 μM of each primer with 2 x of SYBR Green I Roche Diagnostics. The RT-PCR cycling conditions at 95°C for 10 min denaturation step, followed by 40 cycles of 95°C for 15 *s* denaturation, 60 °C for 20 s annealing, and 72°C for 20 *s* elongation steps. Expressed genes data were normalized by GAPDH, as an internal housekeeping control gene.

3. Result and discussion

3.1. X-ray diffraction pattern

The grown prepared powder was analyzed via XRD pattern, which describes the particles crystalline property, crystallite size and phases of the prepared material (Fig. 1). The prepared powder materials XRD, illustrates the peaks, which show the crystalline and phases of the material. The spectrum illustrates the indexed and assigned peaks such as 25.96 < 100 > , 27.78 < 002 > , 28.75 < 101 > , 40.38 < 102 > , 44.62 < 110 > , 51.53 < 103 > and 56.98 < 112 > which are very similar and represents for the formation of Nd_2O_3 and in accordance with hexagonal structure of Nd_2O_3 (JCPDS card no.41–1089) [47]. From the X-ray diffraction pattern, phases, peaks positions, FWHM, crystallite size and average diameter of the crystallite (nm) of the grown powder were calculated with well-known scherrer formula as previously described in the literature [47,48]. The average crystallite was ~17 nm calculated from Scherrer equation as described previously [47,48]. The sharp and intense peaks indicate that the synthesized powder particles exhibit

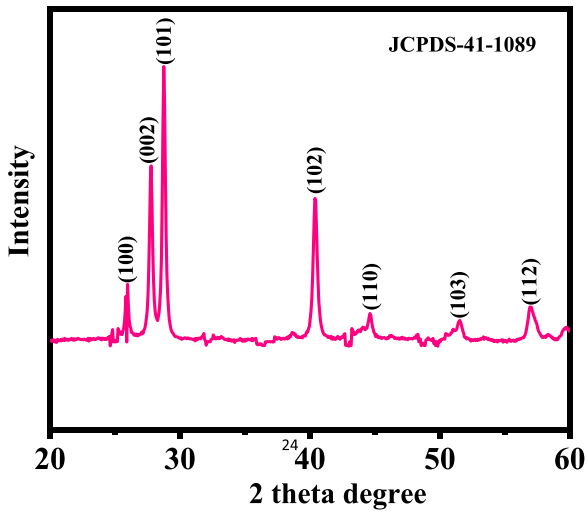

Fig. 1. XRD pattern of the prepared curved shaped nanostructure of neodymium oxide (Nd_2O_3).

good crystallinity, whereas FWHM or wide width of the peaks defined that the size of each crystallite is very small. In the spectrum, no any chemical impurities were observed, which further confirm that the prepared powder is highly pure material.

3.2. Scanning electron microscopy (SEM) results

The identification of processed powders morphology was accomplished with using SEM and the obtained images are illustrated as Fig. 2. From the low magnified images (Fig. 2a-b) seems several particles with dense structures were arranged embedded with the accumulation of several minute particles are appeared which are linked together. For more clarification and the information of an individual particles morphology confirmed from high magnification images (Fig. 2c-d). It seems from the images that several plates and sheets like curved structures are appeared, which exhibit the average estimated diameter of each individual particle structure length ranges from 700 to 1 μm whereas the diameter goes up to 100–150 nm (Fig. 2d). The obtained information from SEM and their material analysis is well vindicated and in consistent with the XRD analysis (Fig. 1).

Including to this, the elemental analysis of the prepared material was also observed via EDS spectroscopy in build with SEM micrograph (Fig. 3). It is clearly seen from the obtained EDS spectrum that only shows the neodymium and oxygen peaks appeared in the spectrum, further reveals that the formed structures were made with neodymium and oxygen. Also their atomic mass ratios are oxygen (20.09%) and neodymium (79.91%). The spectrum and their % atomic rations further reveals that no any other impurities related to the other elements were detected which again confirm that the synthesized material is pure neodymium oxide (Fig. 3).

3.3. Transmission electron microscopy (TEM) results

Furthermore, for more clear clarification related to the morphology, the formed powder was also examined with TEM as described in material and method and the obtained result is presented as Fig. 4. As per the observation recovered from the SEM images, TEM image is also in consistent with the TEM image. Curved shaped nanostructure (Nd_2O_3) structure of neodymium oxide was appeared. The average size of structure in terms of length goes up to about 700 nm, whereas the diameter is about 140 nm. The recovered image confirms that the structure surfaces are smooth, clear and well analogous with SEM (Fig. 2) images.

3.4. FTIR results

Fig. 5(a). Shows that a peak ranges between 3200 and 3600 cm^{-1} illustrate the H-O-H stretching mode. The peak obtained at 2073 cm^{-1} related to the CO_2 where as an intense peak was observed at 1503 cm^{-1} for O-H molecule (Fig. 5a)). The peak obtained at 1392 cm^{-1} is

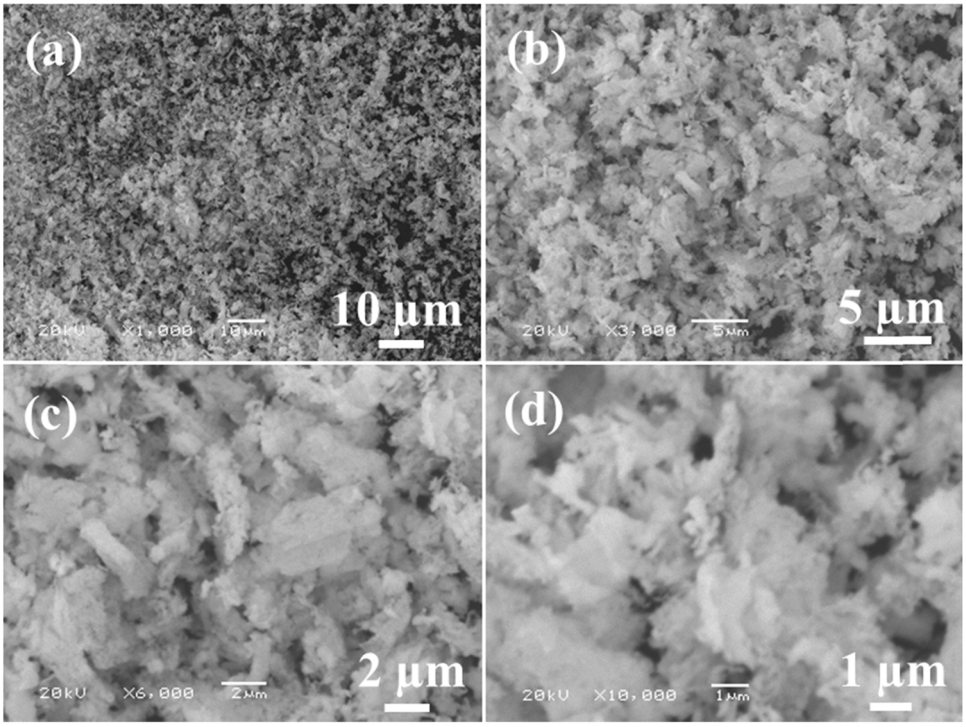

Fig. 2. SEM images of Nd_2O_3 (a-b) shows the low magnification images whereas (c-d) shows the high magnification image at which depicts the surface morphology of the Nd_2O_3.

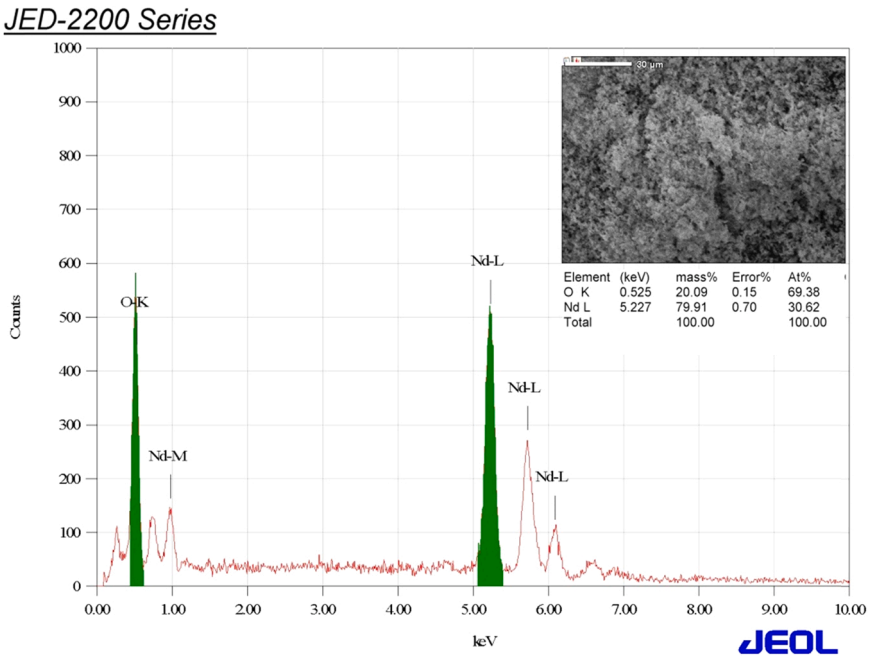

Fig. 3. SEM equipped energy dispersive spectroscopy of Nd_2O_3, which shows the elemental compositions rations of Nd (79.91%) and O (20.09%) respectively.

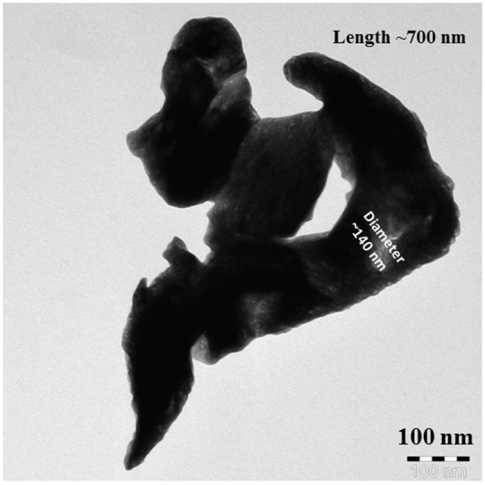

Fig. 4. TEM displayed the average size (diameter and length) of each Nd_2O_3 are ~140–150 and ~700 nm respectively.

correlated to the NO_3^{-1} group [49], whereas the bands at ~680 and 454 cm^{-1} are correlated with the vibration of metal and oxygen bands (Nd_2O_3) respectively [50]. From this spectrum, it demonstrates that there is no any other band was observed related to other functional group in the spectrum, which illustrates the purity of the material [49, 50].

3.5. UV–visible spectroscopy

The UV–visible spectroscopy denotes the optical characteristics of the prepared material. It also signifies the band gap energy of the prepared material. Fig. 6 shows a curved peak at 378 nm wavelength of the prepared material. The band gap value was calculated from the spectrum, which is 3.28 eV (Fig. 5b). This band gap energy is very similar and equal to the observed values as documented in literature [47,51].

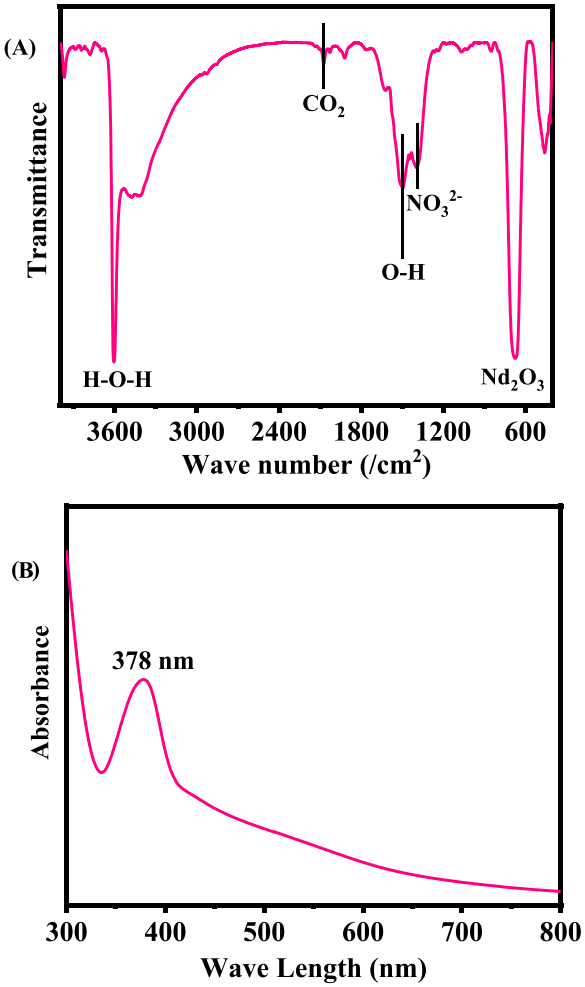

Fig. 5. (A) Typical FTIR spectroscopy of grown Nd_2O_3.**(B)** UV–visible spectroscopy of Nd_2O_3.

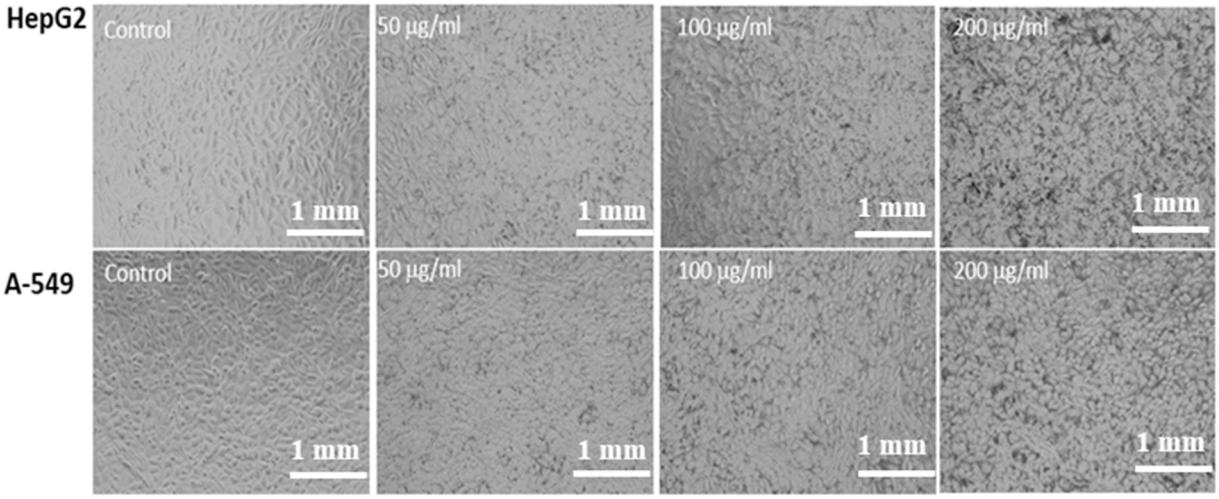

Fig. 6. Morphological changes in HepG2and A-549 cells exposed to various concentrations of Nd_2O_3 for 24 h. Images were taken at 20x (each scale=1 mm).

3.6. Microscopic observations of cancer cells (Hep-G2 and A-549) with Nd_2O_3

The cancer (Hep-G2 and A-549) cells were cultured as described in the materials and method section and their morphological evaluation was observed via microscopy at 24 h incubation periods with a wide range of opted concentrations of Nd_2O_3 (50, 100 and 200 µg/ mL) with control (Fig. 6). From the obtained image, it's evident that it there is no noteworthy alternation was observed at initial range of concentration (50 µg/mL) of Nd_2O_3, but when this concentration was increase to 100 µg/mL, the cells growth was influenced. As can be seen from the recovered images that the growth of cells was much influenced with the processed material and it was dose dependent. At highest concentration of Nd_2O_3 200 µg/mL the cells growth was much affected and morphology of cells was destroyed (Fig. 6). From the microscopic images it's reveals that the cells were completely damaged with the processed Nd_2O_3. Very similar trend is also seen in case of A-549 cells with the Nd_2O_3 with same concentrations (Fig. 6).

3.7. The induced cytotoxicity (MTT Assay) with Nd_2O_3

The cancer cells (HepG2 and A-549 cells) cytotoxicity were examined via MTT assay as mentioned above with different concentrations ranges of material from 2 to 200 µg/mL for 24 h incubation. From the obtained data it shows that viability of cancer cells was diminished with the prepared Nd_2O_3 and the data was concentration/dose-dependent. The HepG2 cells viability, with MTT assay was diminutions at 24 h 100.2%, 100.3%, 96%, 91%, 81%, 73% and 68% (Fig. 7a) for the concentrations of 2, 5, 10, 25, 50 100 and 200 µg/mL respectively ($p < 0.05$ for each). In case of A-549 cells viability, MTT assay was decreases at 24 h 101%, 102%, 100%, 96%, 88%, 81% and 71% (Fig. 7b) for the concentrations of 2, 5, 10, 25, 50 100 and 200 µg/mL respectively ($p < 0.05$ for each). It reveals from the obtained data that initially at low concentration of material much affected whereas once the concentration raises the cytotoxicity of cancer cells were much influenced.

3.8. Cytotoxicity assessment by NRU assay cancer cells with Nd_2O_3

The similar observations were also found in NRU assay as described in the materials and method section. In both utilized cancer cells the prepared materials is not much affected initially, whereas once the concentration or doses of nanostructures increases cells was diminished and it were dose dependent. For the HepG2, NRU assay was decreases at 24 h 99%, 97%, 96%, 90%, 80%, 72% and 64% (Fig. 8a) for the concentrations of 2, 5, 10, 25, 50, 100 and 200 µg/mL respectively

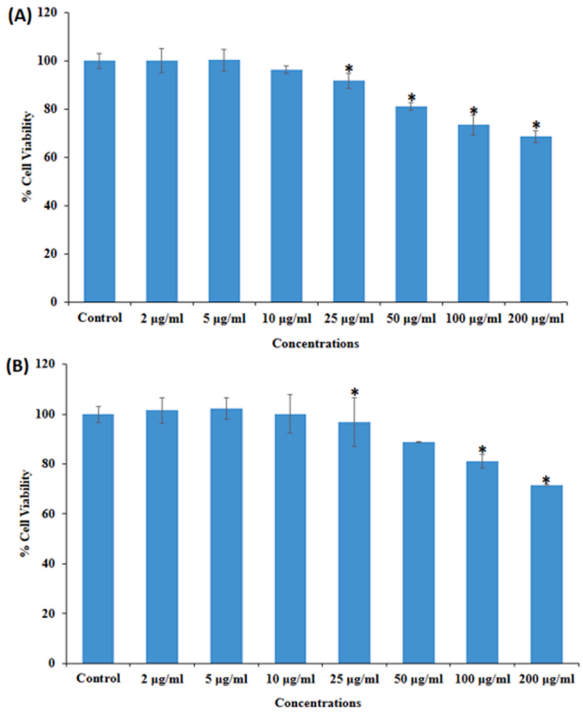

Fig. 7. Percent cell viability by MTT assay in (A) HepG2 and (B) A-549 cells following the exposure of various concentrations of Nd_2O_3 for 24 h. Values are Mean ± SE of three independent experiments.

($p < 0.05$ for each). In case of A-549, NRU assay was decreases at 24 h 99%, 105%, 100%, 105%, 90%, 83% and 73% (Fig. 8b) for the concentrations of 2, 5, 10, 25, 50, 100 and 200 µg/mL respectively ($p < 0.05$ for each).

3.9. Induced ROS generation in cells with Nd_2O_3

A chronological order for ROS generation was examined in case of Hep-G2 cells after the exposure of Nd_2O_3 at 50, 100 and 200 µg/mL concentrations for 24 h (Fig. 9A) with control. As it can be observed from the image (Fig. 9A) and graph (Fig. 9B) that ROS is increases with the increase of Nd_2O_3 as compared to control cells. The ROS were increase at 50 µg/mL, 100 µg/mL and 200 µg/mL were 132, 145, 176% as compared to control (100%) (Fig. 9B).

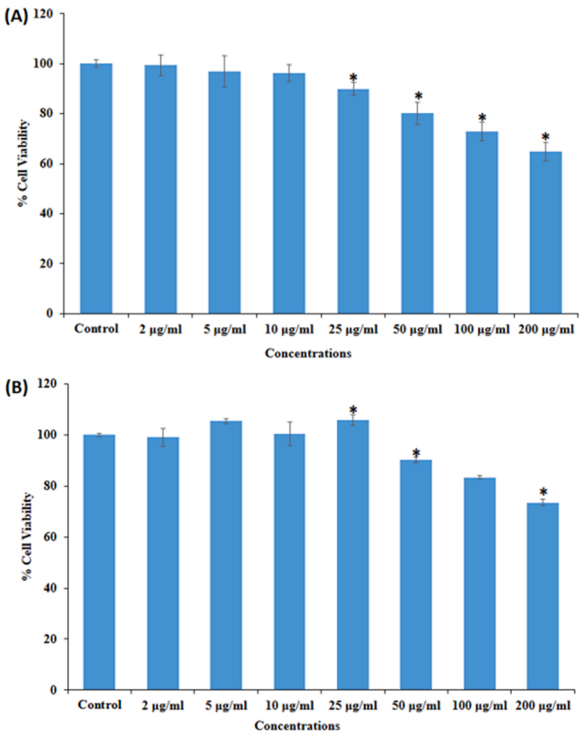

Fig. 8. Percent cell viability by NRU assay in (A) HepG2 and (B) A-549 cells following the exposure of various concentrations of Nd_2O_3 for 24 h. Values are Mean ± SE of three independent experiments.

3.10. *Effect of Nd_2O_3 on cell cycle progression*

The HepG2 cells exposed with 25, 50, 100, and 200 µg/mL of Nd_2O_3 caused an increase in apoptotic (SubG1) phase. The increase in the population of SubG1 phase was observed as 18.2%, 25.2%, 32.2%, and 56% at 25, 50, 100, and 200 µg/mL, as compared to 1.97% in control (Fig. 10). Simultaneously, G2/M phase was reduced from as 17.2%, 16%, 13%, and 8.82% at 25, 50, 100, and 200 µg/mL, relatively, 27.4% G2/M phase was recorded in control.

3.11. *Real time PCR induced by Nd_2O_3*

For the study of mRNA level using quantitative RT-PCR the HepG2 cells were treated to Nd_2O_3 for 24 h at a concentration of 200 µg/mL, and quantitative RT-PCR was performed to evaluate the mRNA level of genes (p53, bax, casp3, and bcl-2). Significantly altered the regulation of apoptotic genes in HepG2 cells ($p < 0.05$ for each gene). The mRNA levels of tumor suppressor gene p53 and the pro-apoptotic gene bax were upregulated. We also identified higher expression of the caspase-3gene in Nd_2O_3 treated cells. The expression of bcl-2, an anti-apoptotic gene, was downregulated in cells treated with Nd_2O_3 (Fig. 11).

4. Discussion

The neodymium oxide (Nd_2O_3), a rare earth element exhibit a remarkable value and largest industrial applications such as powerful permanent magnets, microphones, loud speakers, head phones, electric motors, computer hard disks and various other [52,53]. A series of applications of neodymium [12–20] metal is well described in the literature but very limited applications are available as biological applications and as a nanostructured material. In this study, we have prepared a unique shape and size of neodymium oxide nanostructured material of Nd_2O_3, which seems to be a curved shaped nanostructure (Nd_2O_3). The noteworthy prepared structure was well characterized and confirm with various techniques such as XRD, SEM, and TEM were used to identify the crystallinity, size (D=140 nm and L=~700 nm) and morphology of the synthesized material including the SEM equipped EDX elemental detail. Functional details were confirmed via FTIR spectroscopy and optical activity of the material was examined via UV–visible spectroscopy. Besides the basic information recovered from the characterizations, the main objective of this study was also to investigate the cytotoxic responses of curved shaped nanostructures against liver (HepG2) and lung (A-549) cancer cells. Initially, MTT assay was utilized with and without nanostructures to check the cytotoxicity against cancer cells for 24 h. For to check the viability of cancer cells against the processed material a long range (2, 5,10, 25, 50,100 and 200 µg/mL) of Nd_2O_3 were interacted for 24 h, which shows that the viability cells were in concentration/dose dependent. It is also well evident that the recovered results are in accordance with the previously published literature on cytotoxic activity [54]. It may hypothesize that the cytotoxic activity in both cancer cells with Nd_2O_3 depends upon their unique structural geometry, distinctive property; functions are well responsible for the cell death

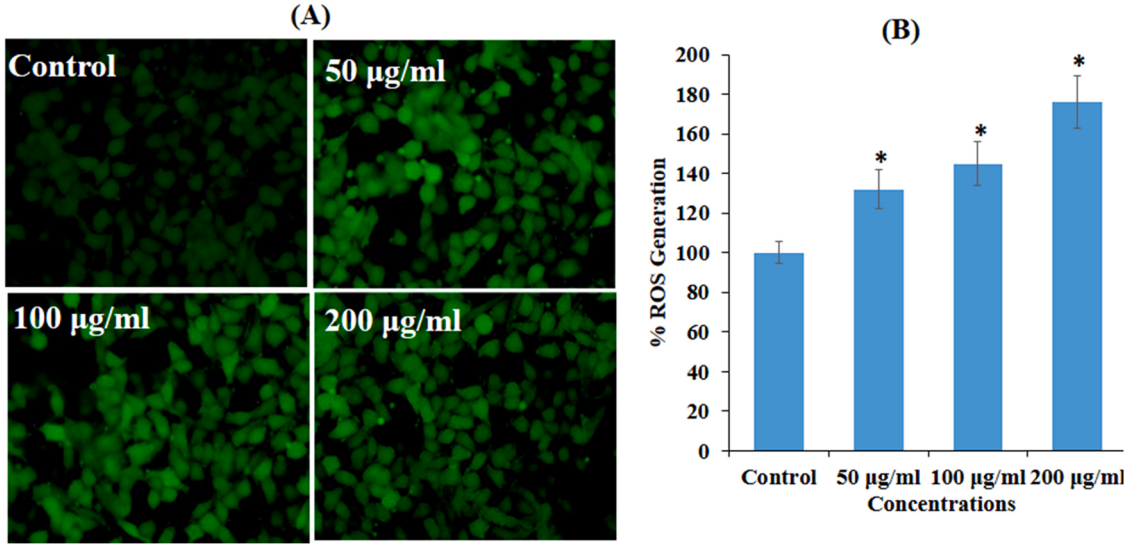

Fig. 9. ROS generation induced by Nd_2O_3 in HepG2 cells exposed for 24 h. where (A) shows the image of ROS generation and (B) displayed their bar diagram. Values are Mean ± SE of three independent experiments.

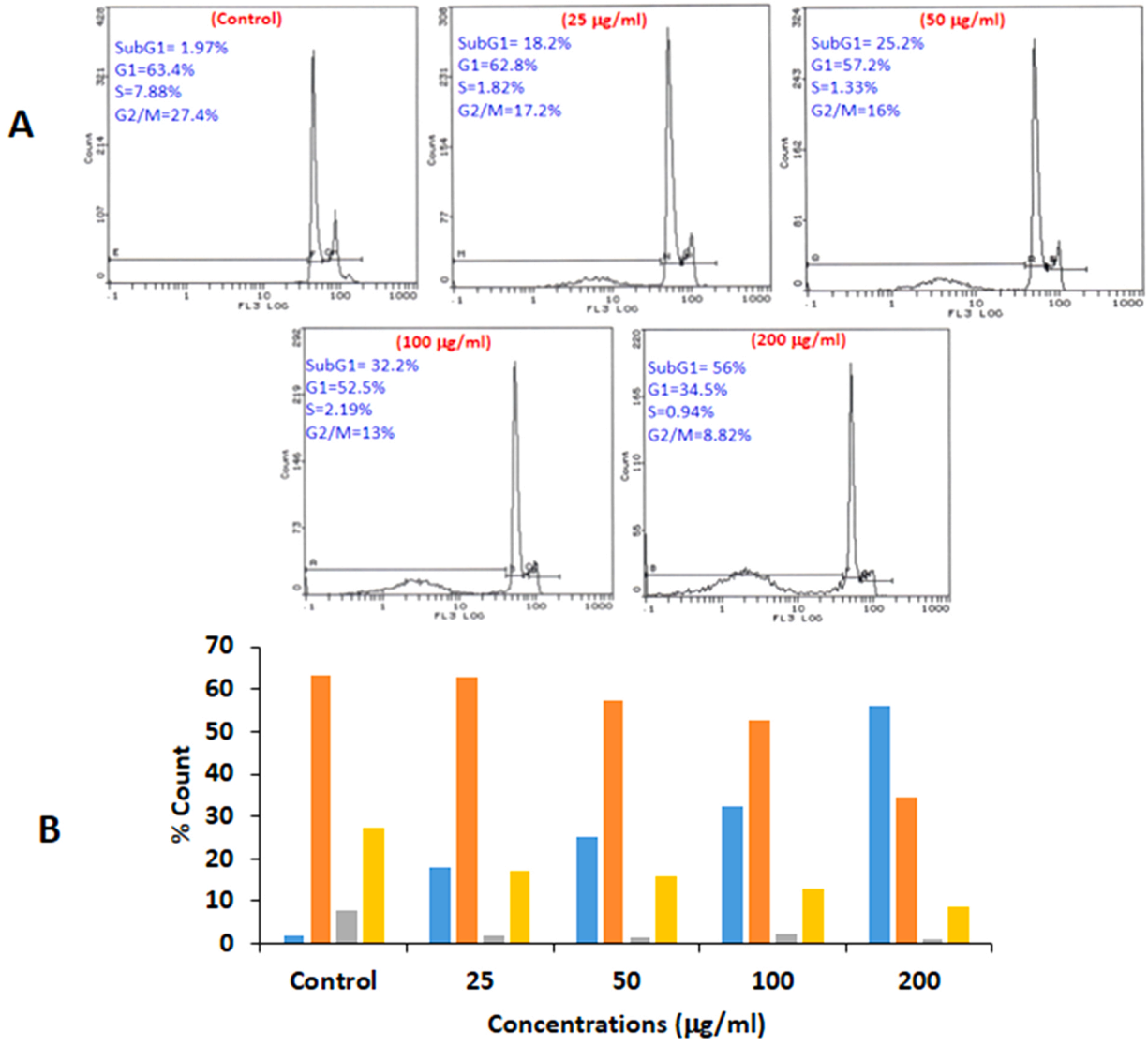

Fig. 10. A and B Cell cycle arrest in HepG2 cells exposed to different concentrations of Nd_2O_3 for 24 h.

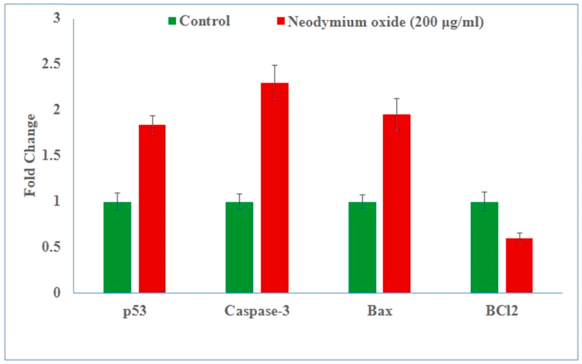

Fig. 11. For mRNA quantification levels, fold change of apoptotic genes (p53, bax, and casp3) and anti-apoptotic gene (bcl-2) was analyzed. Cells treated 200 µg/mL of Nd_2O_3 for 24 h. For the normalization an internal control of GAPDH used. The values are mean ± SE of three independent experiments. *Statistically significant difference as compared to control ($p < 0.05$).

[55]. Further to know the cytotoxicity of cancer cells and the role of Nd_2O_3 with their mechanism, we also measured the reactive oxygen species (ROS), which played a key role for the cytotoxicity in HepG2 and A-549 cells once exposed for 24 h. Apart from the MTT, NRU assays with other physical and chemical parameters, the nanostructured material exhibit the tendency to produce reactive oxygen species (ROS) in cells and are responsible for the toxicological effects [56]. The cells components such as the DNA, protein, and lipids can be possible to disturb their functions with ROS generation and responsible to cell death [57]. The current study showed that Nd_2O_3 persuades the ROS in a quantified dose/concentration-dependent manner in HepG2 and A-549 cells and causes the cell cytotoxicity [58]. The detail study summarizes that the cell death was induced with interaction of Nd_2O_3, resulted the upsurge rate of ROS generation, once treated with nano structures. Based on the received data's such as XRD, SEM, TEM and biological results such as MTT, NRU, and ROS, we may expect that cytotoxicity is dose dependent with their gentle behavior against cancer cells and not to destroyed hardly.

To eradicate the cancer cells completely in human beings a number of therapies were opted such as chemotherapy, radiotherapy etc., but the results are not satisfactory because if any cells remain in the body, it will again grow and form again a giant tumor. Till to date, the surgery is very costly technique and hard for the patients also the recovery is painful and time consuming. Ample work is needed towards this direction to establish a successful ways for to complete reduction of cancer cells at a very low price with efficiently and effectively. The

nanotechnology is now proved and well contributed towards this area at a very cost effective manner. Due to their unique structural organization of nanostructures, facilitates an outstanding improvement to eradicate the cancer cells as equated to the current technologies without any harmful effects. The tiny and unique geometry make a passage to enter easily and quickly to the cancer cells organelles as compared to other existing drugs, which makes possibility to complete reduction of cancer cells.

5. Conclusion

The summary of the present work described here that, we have made curved shaped nanostructures of neodymium oxide via solution process using neodymium nitrate and sodium hydroxide at very low temperature in a very less time. The processed material was well characterized via various applied techniques such as XRD pattern was used to know the crystalline character, phase and particle dimension, reveals that the grown structure is crystalline in nature with free from any other impurities. The morphology of the material was visualized from SEM, which discloses that the prepared material look alike as a curved shaped nanostructure of neodymium oxide with an average size of each particle diameter 140–150 nm whereas the length ranges up to ~700 nm in size. The elemental chemical composition was also confirmed from the SEM equipped EDX, which express the % elemental ratios (oxygen (20.09%) and neodymium (79.91%) in the prepared material. The morphology of the material was further analysed from TEM and it shows that the material seems to be a curved shaped nanostructure (Nd_2O_3) with an average size (Diameter ~140 nm and length ~700 nm) and the obtained data is in consistent with SEM observations. The functional group characteristic were also express that the observed band at ~680 and 454 cm^{-1} are clearly indicates the metal and oxygen bands of Nd_2O_3 respectively, and found that the formed material is pure Nd_2O_3 without any other impurities. In addition to these analysis, the UV–visible spectroscopy data of the prepared material describes that the material is optically active. The efficacy of the material in terms of biological study was also tested against liver (HEPG2) and lung (A-549) cancer cells. The morphological examination of cancer cells (HEPG2 & A-549) were studied via simple microscopy, which reveals that Nd_2O_3 express a moderate and dose dependent effect on cancer cells. The viability of cells was measured via MTT and NRU assays and their obtained results clearly showed that the Nd_2O_3 express their moderate effect against cancer cells as compared to other oxide materials. The unique structures of (Nd_2O_3) exhibit the capability to enter easily in cells and damaged their internal structures. The ROS production in cancer cells due to Nd_2O_3 revealed that high intensity % ratio (166) was achieved with maximum concentration of Nd_2O_3 with green fluorescence by DCF dye with untreated control (100).

The current work provides a future prospective for the cancer cells studies and description of cytotoxicity study of human cell lines with rare earth elements (Nd_2O_3). The work will be useful to understand and utilize the cheap and inexpensive nanostructures for the eradication of cancer cells because till to date the surgery is option to control the cancer cells which is the highly painful and costly for the deprived and low income families.

CRediT authorship contribution statement

Conceptualization. Dr.Javed Ahmad, Dr. Rizwan Wahab Methodology. Dr.Javed Ahmad, Dr. Rizwan Wahab,Software, Dr. Maqsood A. Siddiqui, Dr. Naushad Ahmad, Nida Nayyar Farshori. Validation. Dr. Maqsood A. Siddiqui, Dr. Rizwan Wahab. Formal analysis, Dr.Quaiser Saquib, Dr. Maqsood A. Siddiqui, Naushad Ahmad, Nida Nayyar Farshori Investigation, Dr.Javed Ahmad, Dr. Rizwan Wahab. Resources, Dr. Abdulaziz A Al-Khedhairy, Dr.Quaiser Saquib. Data curation. Quaiser Saquib, Naushad Ahmad, Nida Nayyar Farshori. Writing - Original Draft, Dr.Javed Ahmad, Dr. Rizwan Wahab. Writing - Review & Editing. Dr. Javed Ahmad, Dr. Rizwan Wahab. Visualization. Dr. Maqsood A. Siddiqui, . Supervision. Dr.Abdulaziz A Al-Khedhairy, Dr.Javed Ahmad . Project administration. Dr.Javed Ahmad. Funding acquisition. Dr. Abdulaziz A Al-Khedhairy, Dr.Javed Ahmad.

Declaration of Competing Interest

The authors declare that they have no known competing financial interests or personal relationships that could have appeared to influence the work reported in this paper.

Acknowledgements

The authors are grateful to the Deanship of Scientific Research, King Saud University for funding through Vice Deanship of Scientific Research Chairs.

References

[1] N. Malhotra, H.S. Hsu, S.T. Liang, M.J.M. Roldan, J.S. Lee, T.R. Ger, C.D. Hsiao, An updated review of toxicity effect of the rareearth elements (REEs) on aquatic organisms, Animals 10 (2020) 1663, https://doi.org/10.3390/ani10091663.
[2] G. Charalampides, K. Vatalis, V. Karayannis, A. Baklavaridis, Environmental defects and economic impact on global market of rare earth elements, IOP Conf. Ser.: Mater. Sci. Eng. 161 (2016), 012069.
[3] S.H. Ali, Social and environmental impact of the rare earth industries, Resources 3 (2014) 123–134.
[4] K.T. Rim, Effects of rare earth elements on the environment and human health: a literature review, Toxicol. Environ. Health Sci. 8 (2016) 189–200.
[5] K.T. Rim, K.H. Koo, J.S. Park, Toxicological evaluations of rare earths and their health impacts to workers: a literature review, Saf. Health Work 4 (1) (2013) 12–26.
[6] M.C. Roco, C.A. Mirkin, M.C. Hersam, Nanotechnology research directions for societal needs in 2020: summary of international study, J. Nanopart. Res. 13 (2011) 897–919.
[7] M. Adabi, M. Naghibzadeh, M. Adabi, M.A. Zarrinfard, S.S. Esnaashari, A. M. Seifalian, R.F. Majidi, H.T. Aiyelabegan, H. Ghanbari, Biocompatibility and nanostructured materials: applications in nanomedicine, Artif. Cells, Nanomed., Bio Technol. 45 (4) (2017) 833–842.
[8] S. Hirano, K.T. Suzuki, Exposure, metabolism, and toxicity of rare earths and related compounds, Environ. Health Perspect. 104 (1996) 85–95.
[9] K.T. Rim, K.H. Koo, J.S. Park, Toxicological evaluations of rare earths and theirhealth impacts to workers: a literature review, Saf. Health Work. 4 (2013) 12–26.
[10] D.H. Raymond, R.J. David, in: D.H. Raymond, M.B. Marie, T.J. Giffe (Eds.), Rare earth metals in Hamilton & Hardy's Industrial Toxicology, John Wiley & Sons, Hoboken, NJ, 2015, pp. 199–204.
[11] S.V. Durán, B. Lapo, M. Meneses, A.M. Sastre, Recovery of neodymium (III) from aqueous phase by chitosan-manganese-ferrite magnetic beads, Nanomaterials 10 (6) (2020) 1204.
[12] S. Kontos, A. Ibrayeva, J. Leijon, G. Mörée, A.E. Frost, L. Schönström, K. Gunnarsson, P. Svedlindh, M. Leijon, S. Eriksson, An overview of MnAl permanent magnets with a study on their potential in electrical machines, Energies 13 (2020) 5549.
[13] A. Lixandru, P. Venkatesan, C. Jönsson, I. Poenaru, B. Hall, Y. Yang, A. Walton, K. Güth, R. Gauß, O. Gutfleisch, Identification and recovery of rare-earth permanent magnets from waste electrical and electronic equipment, Waste Manag. 68 (2017) 482–489.
[14] M. Asadollahzadeh, R. Torkaman, M.T. Mostaedi, A. Hemmati, A. Ghaemi, Efficient recovery of neodymium and praseodymium from NdFeB magnet- leaching phase with and without ionic liquid as a carrier in the supported liquid membrane, Chem. Pap. 74 (2020) 4193–4201.
[15] B. Sprecher, R. Kleijn, G.J. Kramer, Recycling potential of neodymium: the case of computer hard disk drives, Environ. Sci. Technol. 48 (16) (2014) 9506–9513.
[16] D.D. München, H.M. Veit, Neodymium as the main feature of permanent magnets from hard disk drives (HDDs), Waste Manag. 61 (2017) 372–376.
[17] S.J.M. Rosid, S. Toemen, W.A.W.A. Bakar, A.H. Zamani, W.N.A.W. Mokhtar, Physicochemical characteristic of neodymium oxide-based catalyst for in-situ CO_2/H_2 methanation reaction, J. Saudi Chem. Soc. 23 (3) (2019) 284–293.
[18] T. Junne, N. Wulff, C. Breyer, T. Naegler, Critical materials in global low-carbon energy scenarios: the case for neodymium, dysprosium, lithium, and cobalt, Energy 211 (2020), 118532.
[19] H.S. Na, S.Y. Ahn, Y.L. Lee, K.J. Kim, W.J. Jang, J.O. Shim, H.S. Roh, The role of additives (Ba, Zr, and Nd) on Ce/Cu/Al_2O_3 catalyst for water-gas shift reaction, Inter, J. Hydrog. Energy 45 (46) (2020) 24726–24737.
[20] T.D. Flierdt, L.F. Robinson, J.F. Adkins, Deep-sea coral aragonite as a recorder for the neodymium isotopic composition of seawater, Geochim. Et. Cosmochim. Acta 74 (21) (2010) 6014–6032.

[21] K. Frohlich, R. Luptak, E. Dobrocka, K. Husekova, K. Cico, A. Rosova, M. Lukosius, A. Abrutis, P. Pisecny, J.P. Espinos, Mater. Sci. Semicond. Process. 9 (6) (2006) 1065–1072.

[22] T. Haoliang, J. Guo, L. Erbao, W. Fuyuan, W. Changliang, G. Mengqiu, G. Junguo, C. Yongjing, Ceram. Int. 46 (1) (2020) 500–507.

[23] R.M..Mohamed, A.A. Ismail, M.W. Kadi, A.S. Alresheedi, I.A. Mkhalid, Photo catalytic performance mesoporous Nd_2O_3 modified ZnO nanoparticles with enhanced degradation of tetracycline, Catalysis Today, ⟨https://doi.org/10.1016/j.cattod.2020.11.002⟩.

[24] K. Suhailath, M. Thomas, M.T. Rame, Article Studies on mechanical properties, dielectric behavior and DC conductivity of neodymium oxide/poly (butyl ethacrylate) nanocomposites, Polym. Polym. Compos. (2020) 1–12.

[25] W. Zhu, J. Ma, L. Xu, W. Zhang, Y. Chen, Controlled synthesis of $Nd(OH)_3$ and Nd_2O_3 nanoparticles by microemulsion method, Mater. Chem. Phys. 122 (2–3) (2010) 362–367.

[26] T. Sreethawong, S. Chavadej, S. Ngamsinlapasathian, S. Yoshikawa, Sol–gel synthesis of mesoporous assembly of Nd_2O_3 nanocrystals with the aid of structure-directing surfactant, Solid State Sci. 10 (1) (2008) 20–25.

[27] B. Huang, C. Huang, J. Chen, X. Sun, Size-controlled synthesis and morphology evolution of Nd_2O_3 nano-powders using ionic liquid surfactant templates, J. Alloy. Compd. 712 (2017) 164–171.

[28] S.H. Jeon, K.N. Hee, J.Y. Young-llKim, D.W. Cho, Y. Sohn, Hydrothermal synthesis of Nd_2O_3 nanorods (Part B), Ceram. Int. 43 (1) (2017) 1193–1199.

[29] W. Yang, Y. Qi, Y. Ma, X. Li, X. Guo, J. Gao, M. Chen, Synthesis of Nd_2O_3 nano powders by sol–gel auto-combustion and their catalytic esterification activity, Mater. Chem. Phys. 84 (1) (2004) 52–57.

[30] S.Z. Ajabshir, S.M. Derazkola, M.S. Niasari, Nd_2O_3-SiO_2 nanocomposites: a simple sonochemical preparation, characterization and photocatalytic activity, Ultrason. Sonochem. 42 (2018) 171–182.

[31] G. Pagano, M. Guida, A. Siciliano, R. Oral, F. Koçbaş, A. Palumbo, I. Castellano, O. Migliaccio, P.J. Thomas, M. Trifuoggi, Comparative toxicities of selected rare earth elements: Seaurchin embryo genesis and fertilization damage with redox and cytogen- etic effects, Environ. Res 147 (2016) 453–460.

[32] C. Blaise, F. Gagné, M. Harwood, B. Quinn, H. Hanana, Ecotoxicity responses of the freshwater cnidarian Hydra attenuata to 11 rare earth elements, Ecotoxicol. Environ. Saf. 163 (2018) 486–491.

[33] N. Duraipandy, M.S. Kiran, Effects of structural distinction in neodymium nanoparticle for therapeutic application in aberrant angiogenesis, Colloids Surf. B: Biointerfaces 181 (2019) 450–460.

[34] H.L. Hua, Y. Huan, S. Xin, G.Y. Rong, X.H. Nan, W.S. Hua, Neodymium oxide induces cytotoxicity and activates NF-κB and Caspase-3 in NR8383 cells, Biomed. Environ. Sci. 30 (1) (2017) 75–78.

[35] Y. Chen, W. Zhu, F. Shu, Y. Fan, N. Yang, T. Wu, L. Ji, W. Xie, R. Bade, S. Jiang, X. Liu, G. Shao, G. Wu, X. Jia, Nd_2O_3 nanoparticles induce toxicity and cardiac/cerebro- vascular abnormality in zebrafish embryos via the apoptosis pathway, Inter. J. Nanomed. 15 (2020) 387–400.

[36] R. Freitas, S. Costa, C.E.D. Cardoso, T. Morais, P. Moleiro, A.C. Matias, A.F. Pereira, J. Machado, B. Correia, D. Pinheiro, A. Rodrigues, J. Colonia, A.M.V.M. Soares, E. Pereira, Toxicological effects of the rare earth element neodymium in *Mytilusgallo provincialis*, Chemosphere 244 (2020), 125457.

[37] A. Alexander, A.S. Pillai, V. Manikantan, G.S. Varalakshmi, B.A. Akash, I.V.M. V. Enoch, Neodymium metal nanorods as camptothecin-carriers, Mater. Lett. 320 (2022), 132326.

[38] C. Rumbo, C.C. Espina, J. Gassmann, O. Tosoni, R.B. García, S.M. Martín, J. A. Tamayo-Ramos, In vitro safety evaluation of rare earth-lean alloys for permanent magnets manufacturing, Sci. Rep. 11 (2021). Article number: 12633.

[39] V.M. Lu, F. Crawshay-Williams, B. White, A. Elliot, Mark A. Hill, H.E. Townley, Cyto toxicity, dose-enhancement and radiosensitization of glioblastoma cells with rare earth nanoparticles, 2019, Artif. Cells, Nanomed. Biotechnol. 47 (1) (2019) 132–143.

[40] J.F. Perz, G.L. Armstrong, L.A. Farrington, Y.J.F. Hutin, B.P. Bell, The contributions of hepatitis B virus and hepatitis C virus infections to cirrhosis and primary liver cancer worldwide, J. Hepatol. 45 (4) (2006) 529–538.

[41] F.S. Wang, J.G. Fan, Z. Zhang, B. Gao, H.Y. Wang, The global burden of liver disease: the major impact of China, Hepatol. Rev. 60 (2020) 2099–2108.

[42] M.A. Siddiqui, M.P. Kashyap, V. Kumar, A.A. Al-Khedhairy, J. Musarrat, A.B. Pant, Protective potential of trans-resveratrol against 4-hydroxynonenal induced damage in PC12 cells, Toxicol. Vitr. 24 (2010) 1592–1598.

[43] M.A. Siddiqui, G. Singh, M.P. Kashyap, V.K. Khanna, S. Yadav, D. Chandra, A. B. Pant, Influence of cytotoxic doses of 4-hydroxynonenal on selected neurotransmitter receptors in PC-12 cells, Toxicol. Vitr. 22 (2008) 1681–1688.

[44] E. Borenfreund, J.A. Puerner, Toxicity determined in vitro by morphological alterations and neutral red absorption, Toxicol. Lett. 24 (2–3) (1985) 119–124.

[45] G. Fotakis, J.A. Timbrell, In vitro cytotoxicity assays: comparison of LDH, neutral red, MTT and protein assay in hepatoma cell lines following exposure to cadmium chloride, Toxicol. Lett. 160 (2) (2006) 171–177.

[46] J. Zhao, M. Riediker, Detecting the oxidative reactivity of nanoparticles: a new protocol for reducing artifacts, J. Nanopart. Res 16 (7) (2014) 2493.

[47] P. Goel, M. Arora, Mechanism of photoluminescence enhancementand quenching in Nd_2O_3 nanoparticles–ferroelectric liquid crystal nanocomposites, RSC Adv. 5 (2015) 14974–14981.

[48] N. Ekthammathat, A. Phuruangrat, B. Kuntalue, S. Thongtem, T. Thongtem, Prepration of Neodymium hydroxide nanorods and Neodymium oxide nanorods by a hydrothermal method, Dig. J. Nanomater. Biostruct. 10 (2) (2015) 715–719.

[49] S. Ahmadi, L. Mohammadi, A. Rahdar, S. Rahdar, R. Dehghani, C.A. Igwegbe, G. Z. Kyzas, Acid dye removal from aqueous solution by using neodymium (III) oxide nanoadsorbents, Nanomaterials 10 (2020) 556.

[50] S.H. Jeon, K. Nam, H.J. Yoon, Y.I. Kim, D.W. Cho, Y. Sohn, Hydrothermal synthesis of Nd_2O_3 nanorods (Part B), Ceram. Inter 43 (1) (2017) 1193–1199.

[51] G.D. Dhamale, V.L. Mathe, S.V. Bhoraskar, S.N. Sahasrabudhe, S.D. Dhole, S. Ghorui, Synthesis and characterization of Nd_2O_3 nanoparticles in a radiofrequency thermal plasma reactor, Nanotech 27 (2016), 085603.

[52] M.S. Lembang, Y. Yulizar, S. Sudirman, D.O.B. Apriandanu, A facile method for green synthesis of Nd_2O_3 nanoparticles using aqueous extract of *Terminalia catappa* leaf, AIP Conf. Proc. 2023 (2018), 020093.

[53] S. Duhan, P. Aghamkar, M. Singh, Synthesis and characterization of neodymium oxide in silica matrix by solgel protocol method, Article ID 237023, Res. Lett. Phys. (2008). Article ID 237023.

[54] Y.S. Kim, C.H. Lim, S.H. Shin, J.C. Kim, Twenty-eight-day repeated inhalation toxicity study of nano-sized neodymium oxide in male sprague-dawley rats, Toxicol. Res 33 (3) (2017) 239–253.

[55] K.T. Rim, K.H. Koo, J.S. Park, Toxicological evaluations of rare earths and their health impacts to workers: a litrature review, Saf. Health Work 4 (2013), 12-12.

[56] F.S. Wang, J.G. Fan, Z. Zhang, B. Gao, H.Y. Wang, The global burden of liver disease: the major impact of China, Hepatol. Rev. 60 (2020) 2099–2108.

[57] J. Ahmad, H.A. Alhadlaq, A. Alshamsanc, M.A. Siddiquia, Q. Saquib, S.T. Khan, R. Wahab, A.A. Al-Khedhairy, J. Musarrat, M.J. Akhtar, M. Ahamed, Differential cytotoxicity of copper ferrite nanoparticles in different human cells, J. Appl. Toxicol. 36 (10) (2016) 1284–1293.

[58] J. Ahmad, R. Wahab, M.A. Siddiqui, Q. Saquib, A.A. Al-Khedhairy, Cytotoxicity and cell death induced by engineered nanostructures (quantum dots and nano particles) in human cell lines, J. Biol. Inorg. Chem. 25 (2020) 325–338.